

RESEARCH ARTICLE | JANUARY 16 2025

# Electron emission performance analysis and application of carbon nanotube cold cathode prepared by cold pressing process

Sheng Lai ; Huaping Tang ; Xin Jin ; Jinsong Pan ; Huan Li ; Yunpeng Liu ; Xiaobin Tang  



*J. Vac. Sci. Technol. B* 43, 013201 (2025)

<https://doi.org/10.1116/6.0004182>



## Articles You May Be Interested In

Fabrication and characteristics of double-gate zinc oxide nanowire field emitter arrays

*J. Vac. Sci. Technol. B* (November 2024)

Continuous synthesis of aligned carbon nanotube arrays on copper substrates using laser-activated gas jet

*Appl. Phys. Lett.* (November 2018)

Systematic growth of carbon nanotubes on aluminum substrate for enhanced field emission performance

*J. Vac. Sci. Technol. B* (February 2021)



## Instruments for Advanced Science



- Knowledge
- Experience
- Expertise

[Click to view our product catalogue](#)

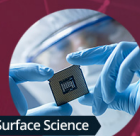
Contact Hiden Analytical for further details:

[www.HidenAnalytical.com](http://www.HidenAnalytical.com)  
[info@hiden.co.uk](mailto:info@hiden.co.uk)



### Gas Analysis

- ▶ dynamic measurement of reaction gas streams
- ▶ catalysis and thermal analysis
- ▶ molecular beam studies
- ▶ dissolved species probes
- ▶ fermentation, environmental and ecological studies



### Surface Science

- ▶ UHV-TPD
- ▶ SIMS
- ▶ end point detection in ion beam etch
- ▶ elemental imaging - surface mapping



### Plasma Diagnostics

- ▶ plasma source characterization
- ▶ etch and deposition process reaction kinetic studies
- ▶ analysis of neutral and radical species



### Vacuum Analysis

- ▶ partial pressure measurement and control of process gases
- ▶ reactive sputter process control
- ▶ vacuum diagnostics
- ▶ vacuum coating process monitoring

# Electron emission performance analysis and application of carbon nanotube cold cathode prepared by cold pressing process

Cite as: J. Vac. Sci. Technol. B 43, 013201 (2025); doi: 10.1116/6.0004182

Submitted: 4 November 2024 · Accepted: 30 December 2024 ·

Published Online: 16 January 2025



Sheng Lai,<sup>1,2,a)</sup> Huaping Tang,<sup>3</sup> Xin Jin,<sup>2</sup> Jinsong Pan,<sup>1</sup> Huan Li,<sup>4</sup> Yunpeng Liu,<sup>1</sup>   
and Xiaobin Tang<sup>1,a)</sup>

## AFFILIATIONS

<sup>1</sup>Department of Nuclear Science and Technology, Nanjing University of Aeronautics and Astronautics, Nanjing 210016, China

<sup>2</sup>NuRay Technology Co., Ltd., South Block, No.6 Building, 1668 Huacheng Rd, Jintan, Changzhou, Jiangsu 213200, China

<sup>3</sup>Department of Engineering Physics, Tsinghua University, Beijing 100084, China

<sup>4</sup>Xi'an Rare Metal Materials Institute Co., Ltd., Xi'an 710016, China

<sup>a)</sup>Authors to whom correspondence should be addressed: laisheng@nuaa.edu.cn and tangxiaobin@nuaa.edu.cn

## ABSTRACT

In this work, a carbon nanotube (CNT) cold cathode electron emitter fabricated by the cold pressing process was developed and studied. The electron emission performance was investigated and the application of pulse x-ray emission and imaging was explored by this cold cathode. The results indicated that the electron emission performance was excellent with electric intensities of turn-on and threshold of 0.47 and 1.17 V/ $\mu\text{m}$  @ 1 mA/cm<sup>2</sup>, respectively, and the field enhancement factor reached 17 514. The application research results showed that the pulse x-ray waveform has a great corresponding well with the grid voltage, and the imaging of a screw was clear, whose thread and pitch could be seen clearly. This article proposed a cold pressing process prepared for the CNT cold cathode, providing a new technical approach for the development of field emission cold cathode preparation processes.

Published under an exclusive license by the AVS. <https://doi.org/10.1116/6.0004182>

## I. INTRODUCTION

Field emission cold cathode electron sources have received widespread attention due to their unique advantages, such as high emission current, instantaneous emission, easy control, no need heating, and low power consumption.<sup>1–4</sup> There are many materials suitable for field emission, including carbon nanotube (CNT), graphene, lanthanum hexaboride (LaB<sub>6</sub>), oxides, etc.<sup>5–8</sup> CNT has great advantages as a field emission material due to its extremely high aspect ratio, stable chemical properties, excellent thermal conductivity, and high-strength mechanical properties.<sup>9,10</sup> Hence, CNT is commonly used as a field emission material. The emission current is affected by the electric field, thermal conductivity, and mechanical strength of field materials in actually.

At present, the popular processes for preparing CNT cold cathode electron sources include screen print, chemical vapor deposition (CVD), spray coating, and electrophoretic deposition. Many scientists have also carried out cold cathode preparation process

research in the past. Zou *et al.*<sup>11</sup> used a NaCl electrolyte to treat CNT emitters prepared by screen print. The result showed that NaCl electrolyte can effectively improve electron emission performance, and the turn-on electric field intensity decreases from 2.2 to 1.6 V/ $\mu\text{m}$ . Park *et al.*<sup>12</sup> prepared CNT cold cathode electron sources using the plasma enhanced CVD method and the emission current density of 1 mA/cm<sup>2</sup> was obtained at 4.05 V/ $\mu\text{m}$  with a field enhancement factor of 2838. Jeong *et al.*<sup>13</sup> employed the spray coating process to prepare thin multiwall CNT emitters. The results showed that emission current density of 1.52 mA/cm<sup>2</sup> could be obtained at a threshold electric field strength of 3.5 V/ $\mu\text{m}$ . Peng *et al.*<sup>14</sup> prepared CNT cold cathodes using the electrophoretic deposition process, which achieved an emission current density of 3.5 mA/cm<sup>2</sup> at an electric field strength of 2.4 V/ $\mu\text{m}$ .

These preparation processes in essence were still to coat CNT coating on the substrate surface and to adhere firmly CNTs to the substrate by using other accessory materials. However, because of leading into accessory materials, such as binder and organic solvent

04 February 2025 07:43:06

used in screen print and spray coating processes, and material affinity agent used in electrophoretic deposition process, these accessory materials are non-conductive and change the surface morphology of cathode, which will limit and weaken the field electron emission performance of CNTs.

Therefore, this work proposed a cold pressing process for preparing CNT cold cathodes that did not require accessory materials. This cold pressing process referred to directly press the CNT powders onto the substrate without introducing any accessory materials on the substrate surface. First, the electron emission performance of CNT cathodes prepared by this cold pressing process was studied. The application performances of high-frequency pulse x ray and x-ray imaging based on this CNT cold cathode were explored. The research in this work expanded the preparation processes of field emission cold cathode, promoting the development of field emission cold cathode preparation technology.

## II. EXPERIMENT

Figure 1 shows the preparation process and pressing sketch map of CNT cold cathodes. The cold pressing process of preparation CNT cold cathodes was loading tin powder and CNT powder into the cold pressing mold, and then using a pressing machine to press the CNT powder and tin powder into cylindrical blocks. The CNT inside the tin block was unable to emission electron. Thus, in the actual preparation process, the tin powder was first put into the pressing machine as the substrate, and then the CNT powder was put into the machine on the top of tin powder. Finally, loading a huge pressure on the cathodes for shaping by the pressing machine. The CNT powder adhered on the surface of the cylindrical tin block.

In general, in order to obtain a solid tin block, the pressure range of tin powder between tens of MPa and hundreds of MPa is required. In this experiment, the pressure applied to form tin blocks was approximately 150 MPa. Due to the existence of internal gaps in the tin and CNT materials, it is necessary to support an extra pressure to those powders during the process for maintaining a constant pressure in the tin and CNT powder.

In this work, the maintaining time was 5 min and without any pressure fluctuation. After preparation, the CNT cold cathode can be obtained through demolding. The overall shape of the CNT cold

cathode was cylinder in shape, which was consistent with the mold. The CNT cold cathode was divided into two layers. The top of tin cylinder column was covered with a layer of CNT powder without any impurity, which is an electron emitter. The thickness of tin cylinder column was greater than that of the CNT layer, which is the substrate. The diameter of tin cylindrical blocks was 5 mm.

The scanning electron microscope (SEM) image of the surface morphology of this CNT cold cathode is shown in Fig. 2. The CNT filaments were firmly adhered to the surface, and most of the filaments were creeping on the substrate surface. From the SEM image, the CNT surface had several microns to tens of microns' fluctuation, which indicated that the CNT film was relatively

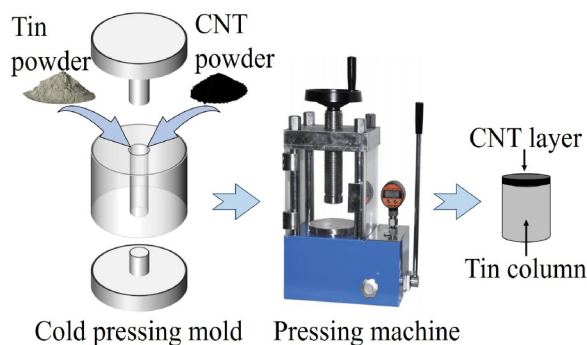


FIG. 1. Preparation process and pressing sketch map.

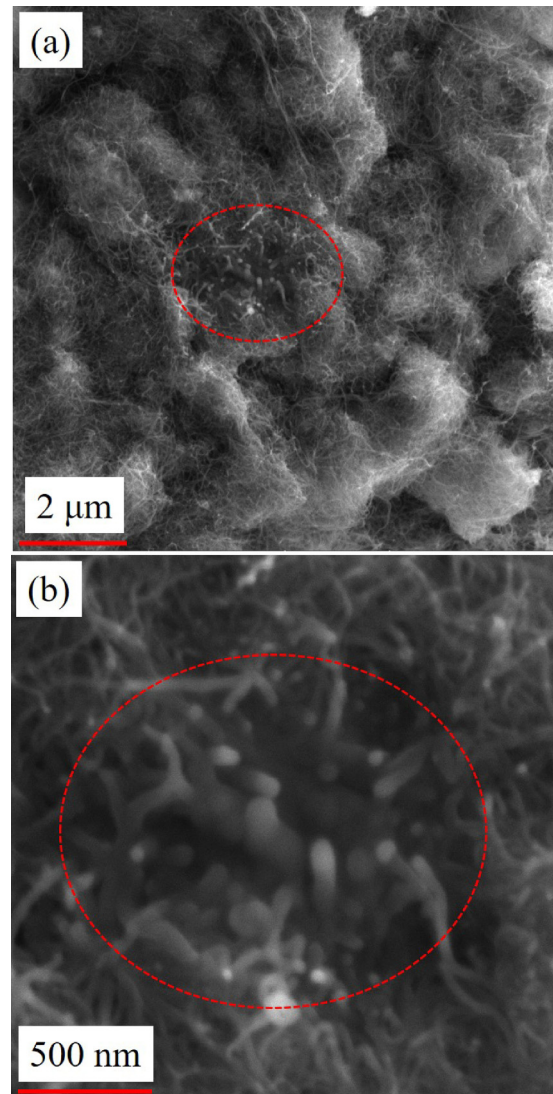


FIG. 2. Characterization of the CNT cold cathode, (a) SEM scale in 2 μm; (b) SEM scale in 500 nm.

04 February 2025 07:43:06

uniform. The CNT diameter was less than 10 nm, and the length was between 5 and 15  $\mu\text{m}$ . Figure 2(b) is an enlarged region of the circle area in Fig. 2(a). A small part of CNT filaments were vertical and extended out of the surface, which is the key part for electron emission, as shown in Fig. 2(b). This was the characteristic of the CNT cold cathode electron source prepared by the cold pressing process.

### III. RESULTS AND DISCUSSION

#### A. Electron emission performance and analysis

In order to study the electron emission performance of the CNT cold cathode prepared by the above cold pressing process, it was placed in a dynamic vacuum system, and the vacuum degree was maintained in the order of  $10^{-6}$  Pa during the experiment, as shown in Fig. 3. The triode structure, namely, anode, grid, and cathode, was employed. The distances of cathode-grid, cathode-anode and grid-anode were approximately 300  $\mu\text{m}$ , 23.3 mm, and 23.0 mm, respectively. The electron transmittance of grid was approximately 80%, which meant that there would be about 20% electrons emitted from cathodes were captured by the grid. The anode is a copper target connected to high-voltage power supply, and the inclination angle of the target is  $15^\circ$ , which is beneficial for the x-ray emission out of from the dynamic vacuum system.

During the experiment, the anode was loaded with 5 kV to prevent the damage of grids and cathodes caused by electron back-flow bombardment, the grid was connected to an adjustable positive power supply, and the cathode was grounded.

Compared the electron emission performance with Ref. 15, the cathode electron emission  $I$ - $V$  curve is shown in Fig. 4(a). The cathode in Ref. 15 was a CNT cold cathode prepared by the screen print process. The test structure and cathode area were the same as Ref. 15. In the cathode preparation process, the gap between cathode and grid was not exactly the same due to the differences of component and preparation process. However, the impact of gap could be eliminated by using electric field intensity, which is the ratio of potential in grid to the gap. Therefore, the

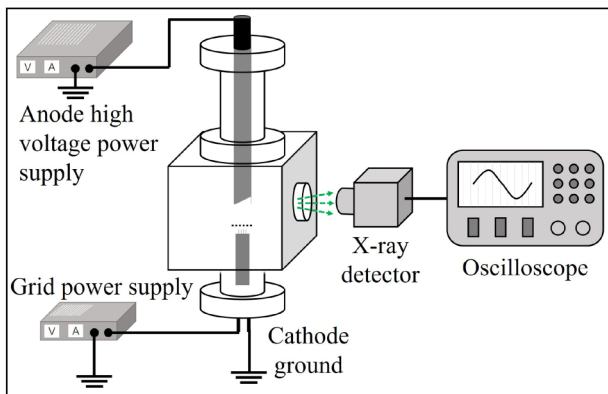


FIG. 3. Measure structure map of the CNT cold cathode in the dynamic vacuum system.

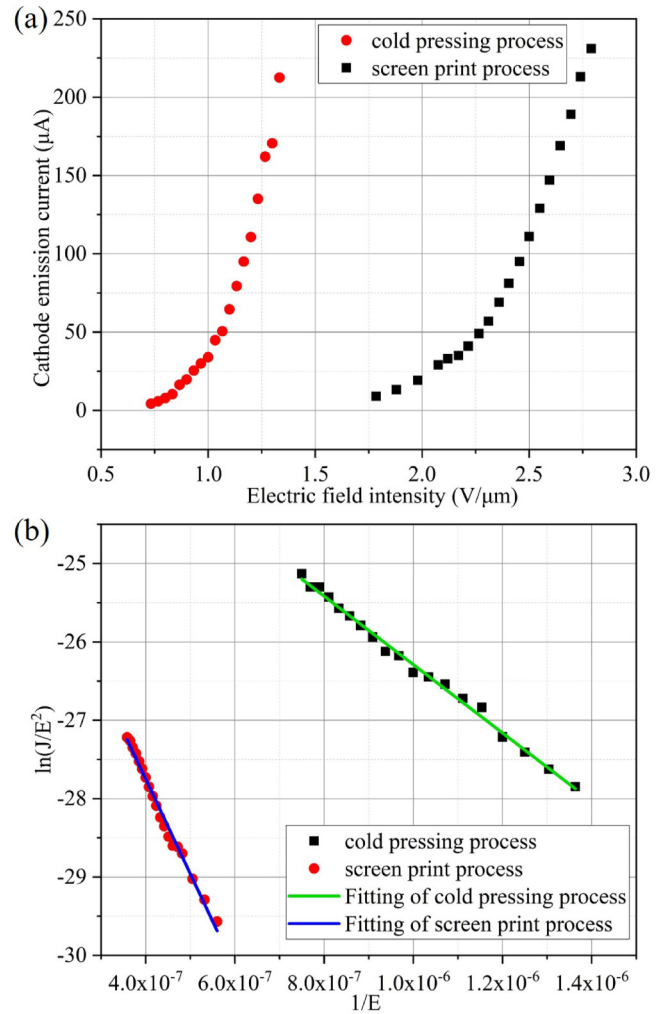


FIG. 4. Electron emission performance of the CNT cold cathode, (a):  $I$ - $V$  characteristics of cathode prepared by the cold pressing process in this work and screen print process in Ref. 15; (b):  $F$ - $N$  theoretical verification by formula (2) and linear fitting for the cold pressing process in this work and the screen print process in Ref. 15.

results of two curves were able to compare in the same electric field intensity.

The electron emission  $I$ - $V$  curve of the cold cathode prepared by the cold pressing process showed an exponential growth trend, and the linear in the  $F$ - $N$  curve was very great, which indicated that the electron emission belonged to the field emission behavior, as shown in Fig. 4.

The electric intensities of turn-on and threshold were 0.47 and 1.17  $\text{V}/\mu\text{m}$  @ 1  $\text{mA}/\text{cm}^2$ , respectively. A cathode emission current of 10  $\mu\text{A}$  could be obtained at an electric field intensity of 0.83  $\text{V}/\mu\text{m}$ . When the electric field intensity reached about 1.17  $\text{V}/\mu\text{m}$ , the cathode emission current increased to 100  $\mu\text{A}$ .

04 February 2025 07:43:06

Correspondingly, the cathode emission currents of 10 and 100  $\mu\text{A}$  in Ref. 15 required electric field intensities of approximately 1.8 and 2.48  $\text{V}/\mu\text{m}$ , respectively.

This comparison result indicated that the electron emission performance of the CNT cold cathode prepared by the cold pressing process was stronger than that of the CNT cold cathode prepared by the screen print process.

The Fowler–Nordheim (F–N) electron emission theoretical formula is<sup>15,16</sup>

$$J = \frac{AE^2}{\phi} \exp\left(-\frac{B\phi^3}{E}\right). \quad (1)$$

After transformation,

$$\ln\left(\frac{J}{E^2}\right) = -B\phi^3 \frac{1}{E} + \ln\left(\frac{A}{\phi}\right). \quad (2)$$

The field enhancement factor  $\beta$  can be derived from (2) as<sup>16–18</sup>

$$\beta = -B \frac{\phi^3}{S}, \quad (3)$$

where  $J$  is the current density,  $E$  is the cathode electric field strength,  $A$  and  $B$  are constants equaled to  $1.54 \times 10^{-6} \text{ A eV V}^{-2}$  and  $6.83 \times 10^3 \text{ V eV}^{-3/2} \mu\text{m}^{-1}$ , respectively.  $\phi$  is the work function of CNT,  $\phi = 5 \text{ eV}$ ,<sup>15</sup>  $S$  is the slope of the straight line fitted to the F–N plot.

The field enhancement factors of this work and Ref. 15 were 17 514 and 7406 calculated by formula (3), respectively.<sup>17</sup> The field enhancement factor of the cold cathode prepared by the cold pressing process was approximately 2.4 times than that prepared by the screen print process, which also explained the reason why the electron emission performance of this work was stronger than that of Ref. 15. The reasons for this difference were analyzed, as shown in the concept diagram in Fig. 5.

Figure 5 shows the concept diagram of surface morphology under different processes prepared for cold cathodes. The processes of screen print and cold pressing used in this study were compared and analyzed. In the process of preparing CNT cold cathode through screen print, an organic binder is required to adhere CNT filaments to the surface of conductive substrate, which are generally nonconductive. Therefore, for the screen print process, there were four situations where CNT filaments on the cathode surface, as shown in Fig. 5(a). (1) CNT filaments were completely buried in the organic binder, and these CNT filaments cannot emit electrons; (2) Although the top of CNT filaments were exposed from the organic binder, the feet of these filaments did not contact with the conductive substrate which could not emit electrons; (3) Although the top of CNT filaments exposed the organic binder and the feet did not contact with the conductive substrate, they were connected to the conductive substrate through other CNT filaments in the binder, as shown in the box of mark 3 in Fig. 5(a). These CNT filaments could emit electrons, but the electron emission was limited by other CNT filaments. (4) The top of the CNT filaments exposed

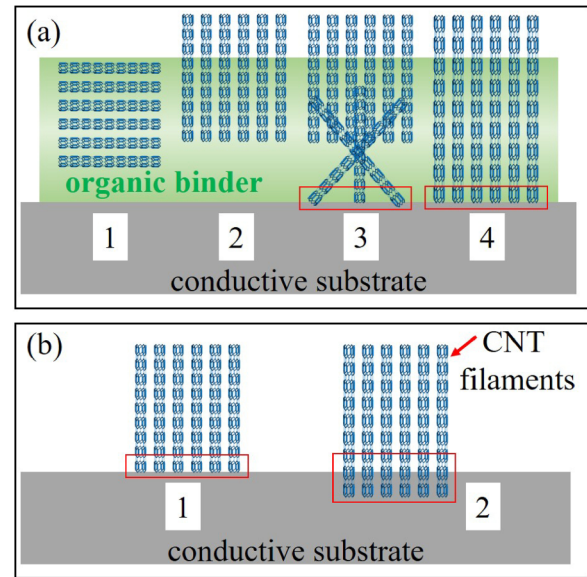


FIG. 5. Concept diagram of surface morphology under different processes prepared for the cold cathode, (a): screen print process; (b): cold pressing process.

the organic binder, and the feet also contacted with the conductive substrate, as shown in the box of mark 4 in Fig. 5(a). These CNT filaments could emit electrons normally.

In comparison, there were two situations on the surface of the CNT cold cathode prepared by the cold pressing process without any accessory materials. (1) The CNT filaments were completely exposed and contacted with the conductive substrate surface, so each CNT filament could emit electrons and had great potential to emit high current. (2) Some CNT filaments were pressed into the tin substrate, which could emit electrons and also increased the contact area between the CNT and the conductive substrate, reducing the Joule heat generated during electron emission and the risk of cathode damage, as shown in the boxes of marks 1 and 2 in Fig. 5(b). Therefore, these reasons could explain why the electron emission performance of the CNT cold cathode prepared by the cold pressing process was stronger than that of the cold cathode prepared by the screen print process, and the cathode prepared by the cold pressing process has a higher field enhancement factor. Compared with the performance of the cold cathode prepared by the screen print process, the cold cathode prepared by the cold pressing process not only emitted electron in a low grid voltage, but also required a lower grid voltage to achieve the same emission current.

## B. Application study of CNT cold cathodes

The application performance of CNT cold cathodes prepared by the cold pressing process was carried out. The pulse x-ray emission characteristics under different pulse emission frequencies were investigated. During the experiment, the grid was connected to a positive constant power supply and the cathode was connected to a

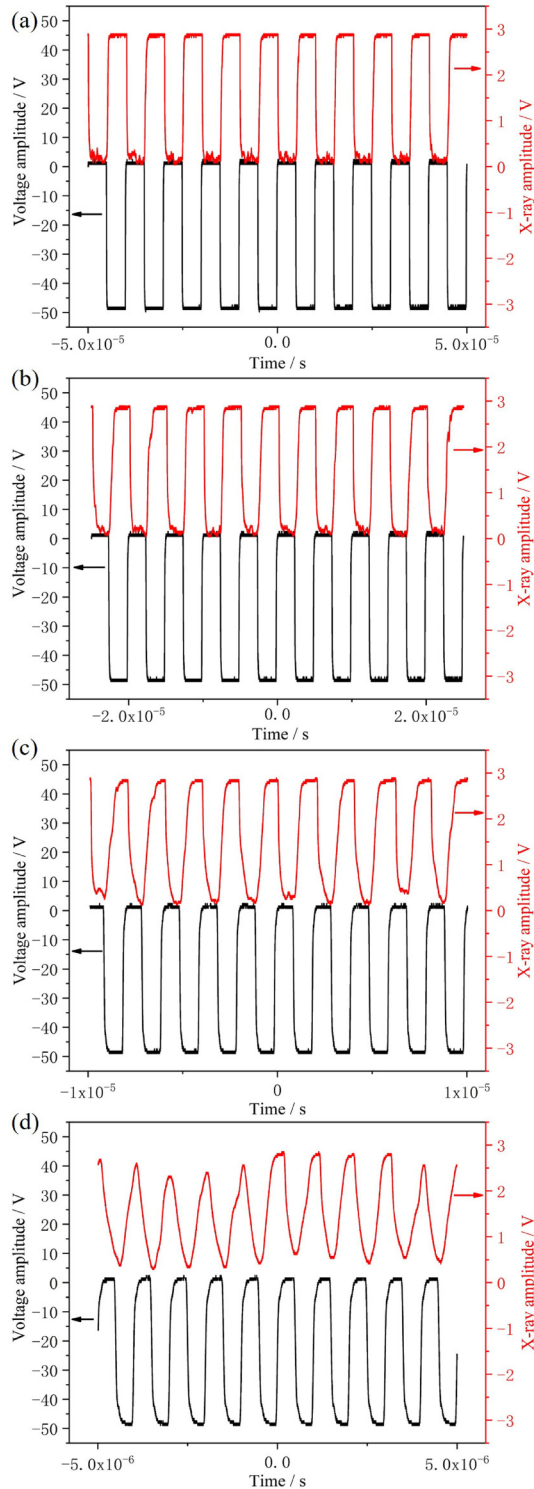


**FIG. 6.** Pulse x-ray waveform, (a) 100 kHz, (b) 200 kHz, (c) 500 kHz, (d) 1 MHz.

negative pulse power supply. In order to obtain sufficient x-ray intensity, the grid voltage was set to 410 V, the maximum pulse voltage amplitude loaded to cathodes was  $-50$  V, and the anode high voltage was set to 25 kV in this study. Under the pulse model, the current was approximately  $250 \mu\text{A}$  and the corresponding resistance was about  $1.8 \text{ M}\Omega$ . The results are shown in Fig. 6. The meanings of left and right axes were cathode pulse voltage and x-ray waveform, respectively. The black and red waveforms were the pulse voltage waveform loaded to the cathode and x-ray waveform, respectively, which were corresponding to the left

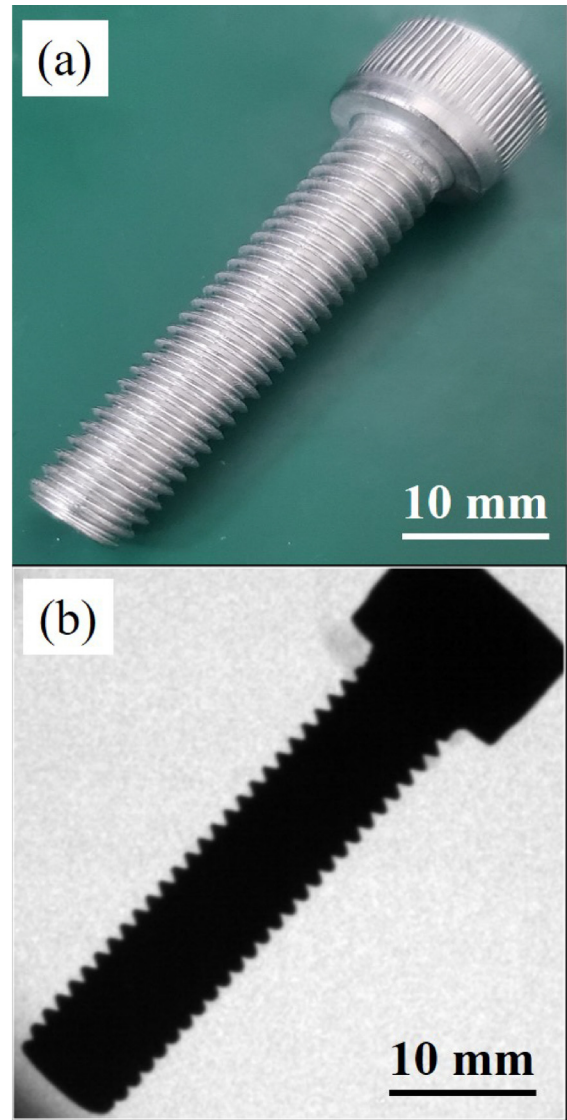


**FIG. 7.** Imaging of a screw based on this CNT cold cathode x-ray source, (a) picture of the actual screw with a size of M8  $\times$  35; (b) x-ray imaging of this screw.

04 February 2025 07:43:06

**TABLE I.** Imaging parameters of the x-ray detector.

Imaging parameters	Value
Detector type	CMOS
Pixel size	100 $\mu\text{m}$
Pixel matrix	1280 $\times$ 1280
Effective area	128 $\times$ 128 $\text{mm}^2$
Frame rate	$\geq 30$ fps@1 $\times$ 1; $\geq 110$ fps@2 $\times$ 2
Effective energy range	below 120 keV

and right ordinates. The x-ray waveform was corresponding well with the grid voltage waveform when the pulse frequency was below 500 kHz, as shown in Figs. 6(a) and 6(b). When the grid voltage waveform was at low level, the x-ray waveform was at high level; Correspondingly, when the grid voltage waveform was at high level, the x-ray waveform was at low level. When the pulse frequency reached 1 MHz, there was a mismatch between the grid voltage waveform and the x-ray waveform, which was caused by delay time.

The reasons and factors that caused delay time were described in detail in Ref. 19. This pulse experiment demonstrated that this CNT cold cathode could serve as a pulse electron source, achieving pulse electron emission and obtaining pulse x-ray waveform in high-frequency, as shown in Figs. 6(c) and 6(d). It could be applied in applications such as x-ray communication and high-speed x-ray imaging.<sup>20–22</sup>

In order to evaluate the imaging performance based on this CNT cold cathode prepared by the cold pressing process, an x-ray imaging experiment of a screw was carried out. The experimental results are shown in Fig. 7. In this study, a screw with a size of M8  $\times$  35 was selected for carrying out x-ray imaging, as shown in Fig. 7(a).

The imaging equipment was Merak-1313 produced by Sensview Technology (Chengdu) Co., Ltd. The imaging parameters of this detector are shown in Table I. The x-ray detector Merak-1313 was placed in front of the x-ray window with a 15 cm distance, as shown in Fig. 3. During the x-ray imaging experiment, the anode was loaded to 32 kV high voltage with an approximately 150–200  $\mu\text{A}$  adjusted through imaging quality in the DC model, and the cathode was grounded. The imaging results were shown in Fig. 7(b). From Fig. 7(b), an image of the screw was obvious exceedingly, and the thread and pitch of the screw could be clearly seen. It indicated that the CNT cold cathode x-ray source prepared by the cold pressing process was feasible for x-ray imaging, and the imaging quality was excellent.

#### IV. CONCLUSION

This work proposed a cold pressing process for CNT cold cathodes, and the performances of electron emission and practical application were researched. The preparation of the CNT cold cathode by the cold pressing process had advantages of simple operation and low cost. Compared to the CNT cold cathode prepared by the screen print process, the CNT cold cathode prepared by the cold pressing process had stronger electron emission

performance. The electric intensities of turn-on and threshold were 0.47 and 1.17  $\text{V}/\mu\text{m}@1 \text{ mA}/\text{cm}^2$ , respectively, and the field enhancement factor reached 17 514. The pulse x-ray waveform has a great corresponding well with the grid voltage, and the imaging of a screw was clear. The research in this work expanded the preparation processes of field emission cold cathode, thereby promoting the development of field emission cold cathode preparation technology.

#### AUTHOR DECLARATIONS

##### Conflict of Interest

The authors have no conflicts to disclose.

##### Author Contributions

**Sheng Lai:** Conceptualization (lead); Data curation (lead); Formal analysis (lead); Investigation (lead); Methodology (lead); Validation (lead); Writing – original draft (lead); Writing – review & editing (lead). **Huaping Tang:** Conceptualization (equal); Resources (equal). **Xin Jin:** Conceptualization (equal); Resources (equal). **Jinsong Pan:** Conceptualization (equal); Resources (equal). **Huan Li:** Conceptualization (equal); Resources (equal). **Yunpeng Liu:** Conceptualization (equal); Resources (equal). **Xiaobin Tang:** Conceptualization (equal); Resources (equal).

#### DATA AVAILABILITY

The data that support the findings of this study are available from the corresponding authors upon reasonable request.

#### REFERENCES

- Q. L. Liao, Y. Yang, J. J. Qi, Y. Zhang, Y. H. Huang, L. S. Xia, and L. Liu, *Appl. Phys. Lett.* **96**, 073109 (2010).
- J. W. Jeong, J. T. Kang, S. Choi, J. W. Kim, S. Ahn, and Y. H. Song, *Appl. Phys. Lett.* **102**, 023504 (2013).
- S. Park *et al.*, *IEEE Electron Device Lett.* **39**, 1936 (2018).
- Y. Zhang, Y. M. Tan, L. Z. Wang, B. H. Li, Y. L. Ke, M. X. Liao, N. S. Xu, J. Chen, and S. Z. Deng, *Vacuum* **172**, 109071 (2020).
- L. L. Jiang *et al.*, *Adv. Mater.* **25**, 250 (2013).
- A. B. Deore, A. T. Jagdale, C. D. Mistari, K. Jagtap, S. R. Jadhkar, M. A. More, S. R. Gadakh, T. Ueki, and P. M. Koinkar, *Int. J. Mod. Phys. B* **38**, 2440016 (2024).
- P. Kandlakunta, R. Pham, R. Khan, and T. Z. Zhang, *Phys. Med. Biol.* **62**, N320 (2017).
- S. Y. Ding, Y. H. Zhou, M. Ye, and W. Lei, *Vacuum* **139**, 33 (2017).
- J. H. Zhang, C. R. Yang, Y. J. Wang, T. Feng, W. D. Yu, J. Jiang, X. Wang, and X. H. Liu, *Nanotechnology* **17**, 257 (2006).
- B. Sun, Y. Wang, and G. F. Ding, *Opt. Mater. Express* **7**, 32 (2017).
- R. J. Zou, G. N. Zou, C. R. Wang, and S. L. Xue, *Appl. Surf. Sci.* **255**, 8672 (2009).
- S. Park *et al.*, *Nanomaterials* **8**, 378 (2018).
- H. J. Jeong, H. K. Choi, G. Y. Kim, Y. I. Song, Y. Tong, S. C. Lim, and Y. H. Lee, *Carbon* **44**, 2689 (2006).
- Y. T. Peng, Y. Z. Hu, and H. Wang, *Colloids Surf. A* **329**, 161 (2008).
- S. Lai, X. B. Tang, Y. P. Liu, J. X. Mu, Z. P. Feng, and K. Miao, *Nanotechnology* **33**, 075201 (2022).
- A. G. Kolosko, S. V. Filippov, P. A. Romanov, E. O. Popov, and R. G. Forbes, *J. Vac. Sci. Technol. B* **34**, 041802 (2016).

<sup>17</sup>Q. Y. Ji, B. W. Wang, Y. J. Zheng, X. P. Yan, F. G. Zeng, and B. H. Lu, *J. Alloys Compd.* **897**, 163136 (2022).

<sup>18</sup>M. J. Li, Q. L. Wang, J. Xu, J. Zhang, Z. Y. Qi, and X. B. Zhang, *Nanomaterials* **11**, 1810 (2021).

<sup>19</sup>S. Lai, Y. P. Liu, J. X. Mu, Z. Peng, Feng, K. Miao, and X. B. Tang, *Vacuum* **207**, 111658 (2023).

<sup>20</sup>H. Li, X. B. Tang, S. Hang, Y. P. Liu, and D. Chen, *J. Appl. Phys.* **121**, 123101 (2017).

<sup>21</sup>J. X. Mu, X. B. Tang, Y. P. Liu, S. Hang, H. Li, W. Zhou, P. Dang, and S. Lai, *J. X-Ray Sci. Technol.* **28**, 187 (2020).

<sup>22</sup>W. Lei, Z. Y. Zhu, C. Y. Liu, X. B. Zhang, B. P. Wang, and A. Nathan, *Carbon* **94**, 687 (2015).